Sens-Schönfelder, C., Eulenfeld, T. (2019): Probing the in situ Elastic Nonlinearity of Rocks with Earth Tides and Seismic Noise. - *Physical Review Letters*, *122*, 13.

DOI: http://doi.org/10.1103/PhysRevLett.122.138501

Editors' Suggestion | Featured in Physics

Probing the *in situ* Elastic Nonlinearity of Rocks with Earth Tides and Seismic Noise

Christoph Sens-Schönfelder*
Helmholtz Centre Potsdam—GFZ German Research Centre for Geosciences, Potsdam, 14473, Germany

Tom Eulenfeld
Institute of Geosciences, Friedrich Schiller University Jena, Jena, 07749, Germany

(Received 9 October 2018; published 5 April 2019)

Heterogeneous materials such as rocks, concrete, and granular materials exhibit a strong elastic nonlinearity. The sensitivity of the elastic nonlinearity to the applied stress and pore pressure in principle allows the use of seismic waves for remote observations of stress or pore pressure changes. Yet the nonlinearity of rocks is difficult to quantify *in situ* as active deformation tests are not possible in the field. We investigate the elastic nonlinearity in a fully natural experiment using the ambient seismic noise of a single seismic station to sense changes of the seismic velocity in the subsurface reaching 0.026% in response to the minute deformation caused by various constituents of the tidal forces exerted by the Sun and Moon.

DOI: 10.1103/PhysRevLett.122.138501

Elastic moduli of geomaterials are not constant. Due to the elastic nonlinearity of heterogeneous materials they change with the applied strain. This makes seismic waves, whose velocity depends on the elastic moduli, an ideal tool for the remote monitoring of subsurface stress or strain variations—an observation that is of fundamental importance in underground operations from construction to mining, and for the monitoring of geological processes in volcanoes and fault zones. However, the strain sensitivity of the seismic wave velocity is a parameter that is hard to measure *in situ*. The laboratory approach to probe the sensitivity in an active deformation test cannot be transferred to the field where controlled strain cannot be applied. Using the laboratory estimates for interpretation on the field scale requires access to representative samples and involves significant uncertainty in the upscaling. Here we show that the improved processing of data from a single seismic station allows measurements of the *in situ* strain sensitivity of the seismic wave velocity in a natural experiment that uses the deformation induced by tidal forces as perturbations and the ambient seismic noise to measure the velocity response. We observe multiple tidal constituents, a thermal strain signal induced by temperature variations and nonlinear coupling between tidal and thermal strain perturbations.

By exciting solid earth tides, the Sun and the Moon perform a controlled deformation experiment with the Earth that provides a way to probe the nonlinear elastic properties of geomaterials on a large spatial scale. Detecting the response of the seismic velocity to varying tidal strain is therefore an attractive target that has been approached with active source measurements [1–4] at dedicated experimental facilities. Such measurements can provide very precise observations and a high spectral resolution depending on their duration. Due to the logistic efforts, active source measurements are impractical for long term and spatially extensive field observations. For this task, noise correlation monitoring [5–8] is the ideal tool that uses the ambient vibration field, which is recorded with standard seismometers at thousands of locations globally. However, monitoring tidal deformation with ambient seismic noise has been of limited success so far due to the precision required that to date has only allowed us to distinguish between periods of high and low volumetric strain using arrays of several seismometers [9,10]. Here we report observations of tidally induced seismic velocity changes with unprecedented spectral resolution and precision from a single seismic station in Chile (Patache). These allow us to observe several tidal constituents in the spectrum of the seismic velocity variations which we use to calibrate the velocity-strain sensitivity.

The station Patache (PATCX) of the Integrated Plate Boundary Observatory Chile (IPOC) [11] is located in the Atacama desert in northern Chile. Variations of the seismic velocity have been observed at PATCX following the dynamic deformation during earthquake shaking and in response to the thermal strain caused by annual and daily temperature variations [12,13]. An image of the geological material close to the station and a thin section in Fig. 1 show numerous clasts embedded in a "gypcrete" matrix containing large amounts of evaporites (likely gypsum and halite).

In the present Letter, we use three-component seismic data of PATCX from January 1, 2007 until January 31, 2018.

Variations of seismic velocity.—Calculation of noise correlation functions to retrieve the pulse-echo Green's function and the procedure to measure velocity changes at high precision and temporal resolution are described in

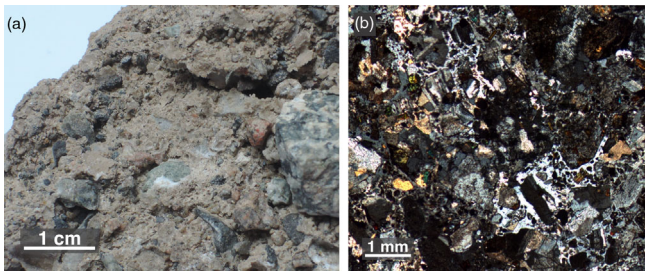

FIG. 1. Geological material at station PATCX in northern Chile. (a) image of sample, (b) thin section.

the sections I and II of the Supplemental Material [14]. It details our new procedure for temporal smoothing and the combination of observations from different components. Figure 2 shows the relative seismic velocity change at station PATCX for 11 years with 10 min sampling. To reduce scatter in the time series, a temporal smoothing of 250 min is applied. We use a 10 s long time window starting at 2 s lapse time in the coda of the noise correlation functions. Figure 2 shows the estimates of dv/v for each individual component combination and for the joint measurement. The most prominent features in the long term time series of Fig. 2(a) are an annual cycle and coseismic velocity decreases during the Tocopilla (2007) and Iquique (2014) earthquakes that are followed by transient velocity increase. The close-up on March 2008 in Fig. 2(b) shows that the broad scatter in the long time series is not a random measurement error but a deterministic signal with a period of about one day. Additionally, the co- and postseismic changes immediately after two small aftershocks of the Tocopilla earthquake are visible.

To investigate the cause of the periodic variations we calculate the spectrum of the jointly estimated velocity changes with a true 10 min resolution. Figure 3 shows the amplitude spectrum of the 11 years of observation of the velocity variations resulting in a frequency resolution of about 2.5×10^{-4} d^{-1}, i.e., 2.9 nHz. The frequency axis is in cycles per day (d^{-1}). The spectrum [Fig. 3(a)] contains a dominant peak at 1 cycle per day and a number of spectral groups roughly located around overtones of the 24 h oscillation. Close-ups of the different groups are shown in panels (b)–(f) of Fig. 3. Supplemental to the velocity, Fig. 3 shows the spectrum of the tidal volume strain calculated with the ETERNA [19] PREDICT program in the same time period.

A broad enlargement of the peaks around 2 d^{-1} in Fig. 3(b) shows two isolated peaks at 1.896 d^{-1} and 1.932 d^{-1}. These peaks correspond to the frequencies of the larger lunar elliptic semidiurnal tide N_2 and the principal lunar semidiurnal tide M_2 [20]. Consequently these peaks are also present in the spectrum of the tidal

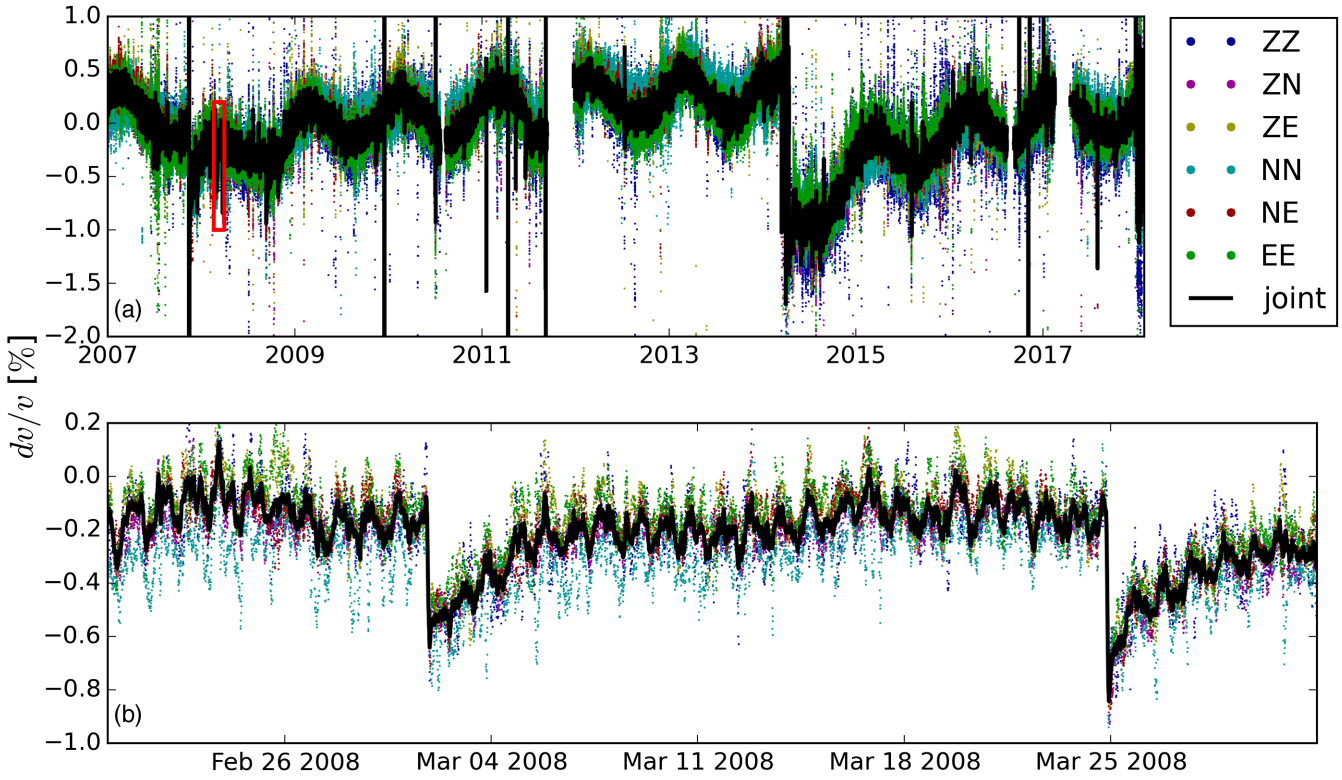

FIG. 2. Seismic velocity variations at station PATCX. (a) Long term velocity variations and (b) enlarged, from February 20 until April 1, 2008, showing the velocity decrease due to two earthquakes and superimposed diurnal and semidiurnal oscillations. Colored dots show results obtained from individual component combinations and black line marks the joint estimate.

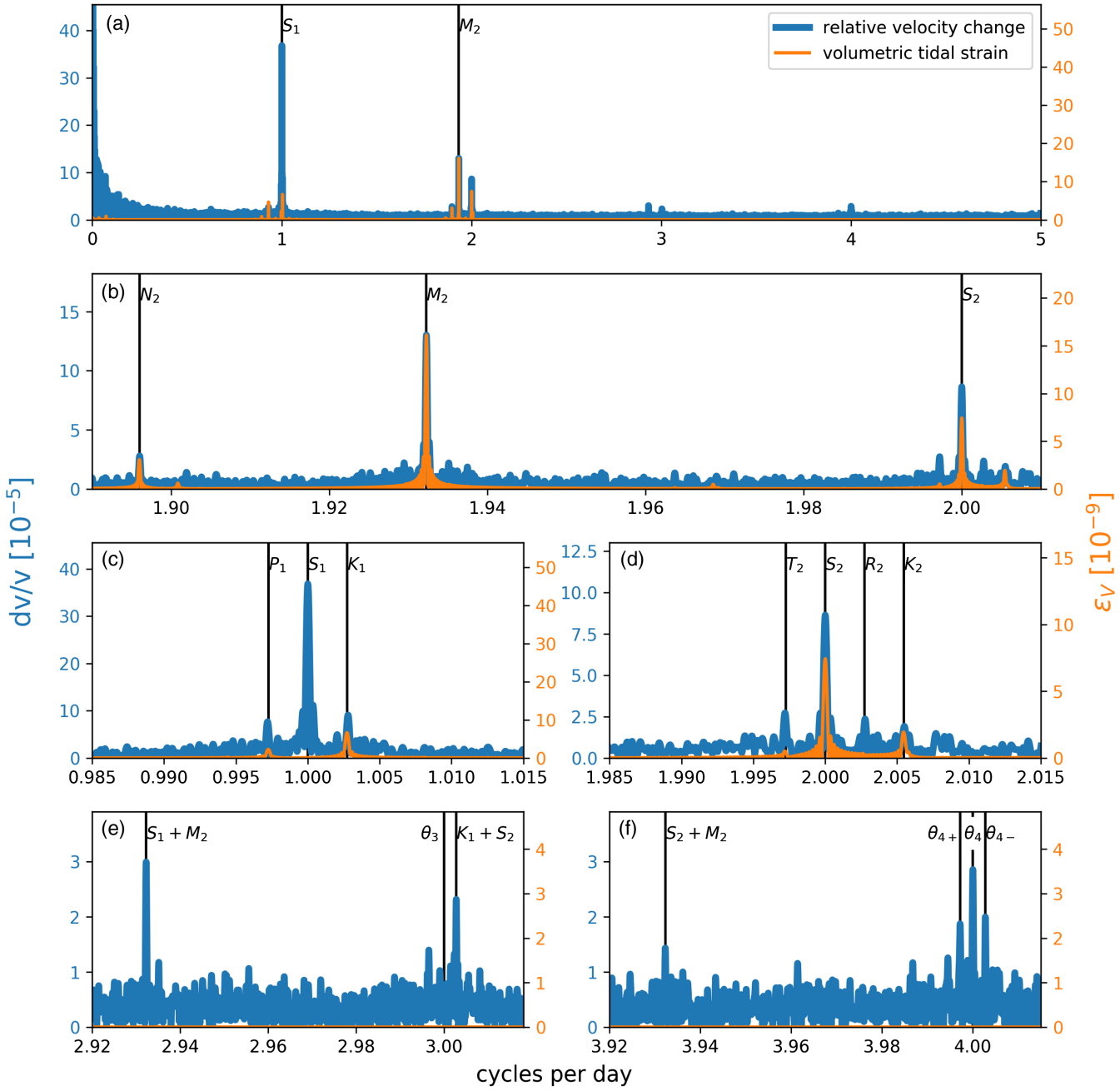

FIG. 3. Spectrum of velocity changes with true 10 min resolution together with volumetric tidal strain. Broad spectrum in (a) shows diurnal and semidiurnal peaks. (b) through (f) show enlarged peaks of one to four cycles per day.

strain signal (orange curve in Fig. 3). The M_2 spectral amplitude of $dv/v = 13 \times 10^{-5}$ corresponds to an average peak to peak velocity change of 0.026%. Another peak is present in the velocity as well as the tidal spectra at exactly 2 d^{-1}. It corresponds to the principal solar semidiurnal tide S_2. Since this cycle can be influenced by tidal strain as well as by thermal strain [12,21,22] and atmospheric pressure variations [23] due to the solar radiation, the ratio of the tidal strain and velocity spectral amplitudes of S_2 differs from that of the lunar constituents. This difference is even stronger for the solar diurnal tide S_1 at 1 d^{-1} [Fig. 3(c)]. The S_1 strain signal is negligible in comparison to the other tidal constituents, but the velocity has a pronounced peak as expected from the sensitivity to thermoelastic strain at PATCX [12].

Influence of tidal strain and temperature.—The different peaks in the spectrum of the seismic velocity variations have different explanations. Signals at frequencies that are solely related to lunar tides (M_2 and N_2) are most likely caused by the direct influence of the tidal strain on the seismic velocities. A linear relation is observed between spectral amplitudes of volumetric strain and velocity variation of the

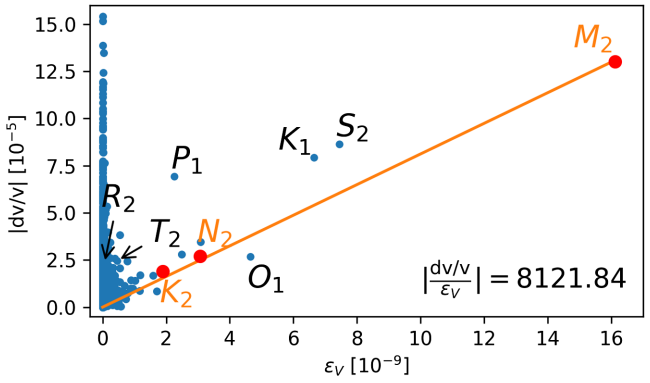

FIG. 4. Velocity sensitivity to tidal strain. Spectral amplitudes of the velocity variations are plotted against volumetric tidal strain for all frequencies. Larger tidal constituents are annotated. Tidal constituents which are not influenced by radiation are highlighted in red. The slope of these points defines the sensitivity of the seismic velocity to changes of the volumetric strain.

tidal constituents N_2, M_2, and K_2 that are not influenced by radiation effects (Fig. 4) defining the absolute value of the sensitivity of seismic velocity to volumetric strain perturbations $|(dv/v)/\epsilon_V| = (8 \pm 2) \times 10^3$ [24]. We estimate the depth sensitivity of these observations to be about 100 m [25]. For plane wave propagation, this sensitivity is related by $\beta \approx 2|(dv/v)/\epsilon_V|$ to the commonly used parameter of quadratic nonlinearity β defined as $M = M_0(1 + \beta\varepsilon)$ with the nonlinear elastic modulus M and the linear elastic modulus M_0.

The velocity does not instantaneously follow the tidal strain. The velocity maximum of M_2 lags 150 ± 15 min behind the volumetric strain minimum (compression, Fig. S1 in the Supplemental Material) [29]. We suggest that this delay results from the transient response of the rocks, which leads to either hysteresis in load experiments [30] or slow dynamic recovery after dynamic perturbations [31]. The transient response can be related to thermally activated processes at weak internal cracks and contacts [32,33].

The phase lag complicates a comparison with other observations that did not allow for a phase shift between strain and velocity [9,10]. At the Pinion Flats Observatory the velocity difference between periods of maximum and minimum strain (0.03%) [10] are close to our peak to peak velocity difference but showed significant differences between observation on different components. A sensitivity of the p-wave velocity to tidal (areal) strain changes of 10^3 was estimated in granite in Japan [4] without a significant phase shift. Since the elastic nonlinearity is considered to arise from processes at grain boundaries and cracks [34], it appears within reason that the sensitivity of the heterogeneous gypcrete in Chile is about eight times larger than that of the Japanese granite. An estimate of the tidal strain sensitivity of seismic velocity at Iwate volcano, Japan [9], of 6.9×10^4 is about ten times larger than our observation—supporting the pronounced susceptibility of volcanic edifices to dynamic perturbations [8]. Velocity changes due to volcanic deformation on a timescale of half a year and longer were used to estimate the strain sensitivity at Izu-Oshima volcano in Japan [35] to be 2.3×10^3. Despite the different timescale, this value is in a similar range as the tidebased observations. It is interesting to note that our strain sensitivity corresponds closely to the acoustic nonlinearity that was used earlier [12] to explain the thermally induced velocity changes at PATCX.

The solar tides are synchronous with the solar radiation and related air pressure and temperature variation that bias the sensitivity $|(dv/v)/\epsilon_V|$ for the cycles at 1 d^{-1}, 2 d^{-1}, 4 d^{-1} (S_1, S_2, θ_4) and their annual modulations (P_1, K_1, T_2, R_2, $\theta_{4+/-}$) in Figs. 3 and 4. The most likely mechanism linking solar radiation to seismic velocity is thermal strain [12,21,22,36]. An exception is the O_1 tidal constituent that is not influenced by radiation but shows an anomaly in the spectral ratios.

In contrast to the tidal strain which is—to first order—constant with depth, daily and annual temperature fluctuations are confined to a very shallow layer. The amplitude of the thermoelastic strain changes in this layer, however, can be orders of magnitude larger than the strain of tidal origin.

Nonlinear coupling of thermal and tidal velocity variations.—In addition to the spectral peaks that can be explained by either tidal strain or thermal effects, we observe further significant peaks in the velocity spectrum. These frequencies [cf. Figs. 3(e) and 3(f)] can be explained exactly by the sum of the frequencies of a solar radiation constituent and a lunar tidal constituent: 2.932 d^{-1} annotated $S_1 + M_2$ is the sum of S_1 and M_2 frequencies, 3.003 d^{-1} ($K_1 + S_2$) is the sum of the lunar diurnal and the solar semidiurnal frequencies and 3.932 d^{-1} ($S_2 + M_2$) equals the sum of the solar and lunar semidiurnal frequencies. This suggests that the thermal and tidal influences on the elastic moduli are not strictly additive but modulate each other to some extent [37].

Discussion.—The deformation experiment that the tidal forces of the Sun and Moon impose on the Earth can be observed with the help of ambient seismic noise recorded at a single seismic station. The high precision observations with temporal resolution below 1 d^{-1} are facilitated by a new processing procedure for noise correlation monitoring. It allows us to observe the velocity response to a dynamic and well characterized natural perturbation—the tidal strain—with high temporal resolution above the timescale of the perturbation. With a single seismometer we are able to conduct *in situ* dynamic acoustoelastic testing [38,39] (DAET) which is currently one of the most elaborate experimental protocols to characterize elastic nonlinearity in terms of both amplitude and phase of the response at the excitation frequency and its overtones [40].

The strain sensitivity observed here is within the range of comparable observations [4,9,10]. However, we show that a significant phase lag can occur between tidal strain and the

velocity response. This possibility was not considered in previous studies that measured the velocity difference between periods of maximum and minimum strain [9,10].

Since tidal strain as a perturbation and seismic noise as a probe are ubiquitous, our approach can be used to gauge the velocity-strain sensitivity of subsurface materials wherever seismic observations of about one month are available [43]. We see three important implications of this development. (1) Ideally, precise knowledge of the velocity strain sensitivity allows quantitative estimates of stress and strain changes to be obtained from seismic measurements. It could turn seismometers into strain meters. (2) Under dry conditions the velocity-strain sensitivity depends on confining pressure [39]. In the presence of pore-fluids we can assume that the velocity-strain sensitivity depends on effective pressure [44,45] providing an alternative means for remote estimation of pore pressure [8,46,47]. Finally (3) the dynamic response of geomaterials (in amplitude and phase) to a controlled perturbation is a novel observation that will contribute to a more complete characterization of subsurface properties and a holistic understanding of transient rheological phenomena such as dynamic softening after earthquakes [8,13,48], transient recovery [13,48], and hysteresis [49] that is not yet developed. Since our observation requires data from a single seismometer only, it is suitable for applications in planetary seismology [50] and may help to probe the subsurface of Mars with seismic data from the inSight mission.

We wish to acknowledge the IPOC consortium for maintaining the station and providing the data. C. S. acknowledges numerous inspiring discussions with Roel Snieder and we thank Robert Green for important comments on the manuscript. We thank Thomas Jahr and Christian Voigt for calculating the tidal strain signal.

*sens-schoenfelder@gfz-potsdam.de

[1] T. L. De Fazio, K. Aki, and J. Alba, Solid earth tide and observed change in the in situ seismic velocity, J. Geophys. Res. **78**, 1319 (1973).

[2] P. A. Reasenberg and K. Aki, A precise, continuous measurement of seismic velocity for monitoring in situ stress, J. Geophys. Res. **79**, 399 (1974).

[3] H. Yukutake, T. Nakajma, and K. Doi, In situ measurements of elastic wave velocity in a mine, and the effects of water and stress on their variation, Tectonophysics **149**, 165 (1988).

[4] K. Yamamura, O. Sano, H. Utada, Y. Takei, S. Nakao, and Y. Fukao, Long-term observation of in situ seismic velocity and attenuation, J. Geophys. Res. Solid Earth **108**, 1 (2003).

[5] C. Sens-Schönfelder and U. Wegler, Passive image interferometry and seasonal variations of seismic velocities at Merapi Volcano, Indonesia, Geophys. Res. Lett. **33**, L21302 (2006).

[6] F. Brenguier, M. Campillo, C. Hadziioannou, N. M. Shapiro, R. M. Nadeau, and E. Larose, Postseismic relaxation along the San Andreas fault at parkfield from continuous seismological observations, Science **321**, 1478 (2008).

[7] C. Sens-Schönfelder and U. Wegler, Passive image interferometry for monitoring crustal changes with ambient seismic noise; Application de l'imagerie passive à la surveillance des modifications de la croûte à partir du bruit sismique ambiant, C. R. Geoscience **343**, 639 (2011).

[8] F. Brenguier, M. Campillo, T. Takeda, Y. Aoki, N. M. Shapiro, X. Briand, K. Emoto, and H. Miyake, Mapping pressurized volcanic fluids from induced crustal seismic velocity drops, Science **345**, 80 (2014).

[9] T. Takano, T. Nishimura, H. Nakahara, Y. Ohta, and S. Tanaka, Seismic velocity changes caused by the Earth tide: Ambient noise correlation analyses of small-array data, Geophys. Res. Lett. **41**, 6131 (2014).

[10] G. Hillers, L. Retailleau, M. Campillo, A. Inbal, J.-P. Ampuero, and T. Nishimura, In situ observations of velocity changes in response to tidal deformation from analysis of the high-frequency ambient wavefield, J. Geophys. Res. Solid Earth **120**, 210 (2014).

[11] GFZ German Research Centre for Geosciences; Institut des Sciences de l Univers-Centre National de la Recherche CNRS-INSU, "IPOC Seismic Network. Integrated Plate boundary Observatory Chile—IPOC".

[12] T. Richter, C. Sens-Schönfelder, R. Kind, and G. Asch, Comprehensive observation and modeling of earthquake and temperature-related seismic velocity changes in northern Chile with passive image interferometry, J. Geophys. Res. **119**, 4747 (2014).

[13] M. Gassenmeier, C. Sens-Schönfelder, T. Eulenfeld, M. Bartsch, P. Victor, F. Tilmann, and M. Korn, Field observations of seismic velocity changes caused by shaking-induced damage and healing due to mesoscopic nonlinearity, Geophys. J. Int. **204**, 1490 (2016).

[14] See Supplemental Material at http://link.aps.org/supplemental/10.1103/PhysRevLett.000.000000 section I and II, which include Refs. [5,8,12,15–18].

[15] L. Krischer, T. Megies, R. Barsch, M. Beyreuther, T. Lecocq, C. Caudron, and J. Wassermann, ObsPy: a bridge for seismology into the scientific Python ecosystem, Comput. Sci. Discovery **8**, 014003 (2015).

[16] C. Hadziioannou, E. Larose, and O. Coutant, Stability of monitoring weak changes in multiply scattering media with ambient noise correlation: Laboratory experiments, J. Acoust. Soc. Am. **125**, 3688 (2009).

[17] C. Sens-Schönfelder, E. Pomponi, and A. Peltier, Dynamics of Piton de la Fournaise volcano observed by passive image interferometry with multiple references, J. Volcanol. Geotherm. Res. **276**, 32 (2014).

[18] C. Sens-Schönfelder, Synchronizing seismic networks with ambient noise, Geophys. J. Int. **174**, 966 (2008).

[19] H.-G. Wenzel, The nanogal oftware: Earth tide data processing package ETERNA 3.30, Bulletin d'Informations Marées Terrestres **124**, 9425 (1996).

[20] A. T. Doodson and H. Lamb, The harmonic development of the tide-generating potential, Proc.R. Soc. Ser. A **3**, 305 (1921).

[21] J. Berger, A note on thermoelastic strains and tilts, J. Geophys. Res. **80**, 274 (1975).

[22] Y. Ben-Zion and P. Leary, Thermoelastic strain in a half-space covered by unconsolidated Material, Bull. Seismol. Soc. Am. **76**, 1447 (1986).
[23] B. Haurwitz and A. D. Cowley, The diurnal and semidiurnal barometric oscillations global distribution and annual variation, Pure Appl. Geophys. **102**, 193 (1973).
[24] See Supplemental Material at http://link.aps.org/supplemental/10.1103/PhysRevLett.122.138501 section III for details on confidence limits.
[25] See Supplemental Material at http://link.aps.org/supplemental/10.1103/PhysRevLett.000.000000 section VIII for a discussion of the depth sensitivity, which includes Refs. [13,26–28].
[26] A. Obermann, T. Planes, E. Larose, C. Sens-Schönfelder, and M. Campillo, Depth sensitivity of seismic coda waves to velocity perturbations in an elastic heterogeneous medium, Geophys. J. Int. **194**, 372 (2013).
[27] J. Xia, R. D. Miller, and C. B. Park, Estimation of near-surface shear-wave velocity by inversion of Rayleigh waves, Geophysics **64**, 691 (1999).
[28] H. Sato, M. Fehler, and T. Maeda, *Seismic Wave Propagation and Scattering in the Heterogeneous Earth*, 2nd ed. (Springer, Heidelberg, 2012), p. 494.
[29] See Supplemental Material at http://link.aps.org/supplemental/10.1103/PhysRevLett.122.138501 section III for details on confidence limits.
[30] C. H. Scholz and S. H. Hickman, Hysteresis in the closure of a nominally flat crack, J. Geophys. Res. **88**, 6501 (1983).
[31] J. a. TenCate, Slow dynamics of earth materials: An experimental overview, Pure Appl. Geophys. **168**, 2211 (2011).
[32] O. O. Vakhnenko, V. O. Vakhnenko, T. J. Shankland, and J. A. TenCate, Soft-ratchet modeling of slow dynamics in the nonlinear resonant response of sedimentary rocks, AIP Conf. Proc. **838**, 120 (2006).
[33] X. Li, C. Sens-Schönfelder, and R. Snieder, Nonlinear elasticity in resonance experiments, Phys. Rev. B—Condens. Matter Mater. Phys. **97**, 144301 (2018).
[34] P. Johnson and A. Sutin, Slow dynamics and anomalous nonlinear fast dynamics in diverse solids, J. Acoust. Soc. Am. **117**, 124 (2005).
[35] T. Takano, T. Nishimura, and H. Nakahara, Seismic velocity changes concentrated at the shallow structure as inferred from correlation analyses of ambient noise during volcano deformation at Izu-Oshima, Japan, J. Geophys. Res. Solid Earth **122**, 6721 (2017).
[36] See Supplemental Material at http://link.aps.org/supplemental/10.1103/PhysRevLett.122.138501 section IV for the phase relation between seismic velocity, temperature and tidal strain, which contains Ref. [12].
[37] See Supplemental Material at http://link.aps.org/supplemental/10.1103/PhysRevLett.122.138501 section V for a discussion of the signal modulation.
[38] G. Renaud, J. Rivière, P. Y. Le Bas, and P. A. Johnson, Hysteretic nonlinear elasticity of Berea sandstone at low-vibrational strain revealed by dynamic acousto-elastic testing, Geophys. Res. Lett. **40**, 715 (2013).
[39] J. Rivière, L. Pimienta, M. Scuderi, T. Candela, P. Shokouhi, J. Fortin, A. Schubnel, C. Marone, and P. A. Johnson, Frequency, pressure, and strain dependence of nonlinear elasticity in Berea Sandstone, Geophys. Res. Lett. **43**, 3226 (2016).
[40] See Supplemental Material at http://link.aps.org/supplemental/10.1103/PhysRevLett.122.138501 section VI for the tidal DAET observation, which contains Refs. [38,41,42].
[41] J. Rivière, G. Renaud, R. A. Guyer, and P. Johnson, Pump and probe waves in dynamic acousto-elasticity: Comprehensive description and comparison with nonlinear elastic theories, J. Appl. Phys. **114**, 054905 (2013).
[42] G. Renaud, J. Rivière, C. Larmat, J. Rutledge, R. Lee, R. Guyer, K. Stokoe, and P. Johnson, In situ characterization of shallow elastic nonlinear parameters with Dynamic Acoustoelastic Testing, J. Geophys. Res. Solid Earth **119**, 6907 (2014).
[43] For a discussion of the required measurement duration, see Supplemental Material at http://link.aps.org/supplemental/10.1103/PhysRevLett.122.138501 section VII.
[44] S. Shapiro, Elastic piezosensitivity of porous and fractured rocks, Geophysics **68**, 482 (2003).
[45] C. M. Sayers, An introduction to velocity-based pore-pressure estimation, Leading Edge **25**, 1496 (2006).
[46] T. Taira, A. Nayak, F. Brenguier, and M. Manga, Monitoring reservoir response to earthquakes and fluid extraction, salton sea geothermal field, Sci. Adv. **4**, e1701536 (2018).
[47] E. J. Chaves and S. Y. Schwartz, Monitoring transient changes within overpressured regions of subduction zones using ambient seismic noise, Sci. Adv. **2**, e1501289 (2016).
[48] M. Hobiger, U. Wegler, K. Shiomi, and H. Nakahara, Coseismic and post-seismic velocity changes detected by Passive Image Interferometry: comparison of one great and five strong earthquakes in Japan, Geophys. J. Int. **205**, 1053 (2016).
[49] R. A. Guyer and P. A. Johnson, Nonlinear mesoscopic elasticity: Evidence for a new class of materials, Phys. Today **52**, 30 (1999).
[50] C. Sens-Schönfelder and E. Larose, Temporal changes in the lunar soil from correlation of diffuse vibrations, Phys. Rev. E **78**, 045601 (2008).